Emission characteristics of a homologous series of bimesogenic liquid-crystal lasers

A. D. Ford, S. M. Morris,* M. N. Pivnenko, C. Gillespie, and H. J. Coles†
Centre of Molecular Materials for Photonics and Electronics, Electrical Engineering Division, Engineering Department, Cambridge University, 9 JJ Thomson Avenue, Cambridge CB3 0FA, United Kingdom
(Received 27 July 2007; published 7 November 2007)

In this study we have fabricated eight different liquid-crystal lasers using the same gain medium but different homologues from the bimesogenic series α-(2′, 4-difluorobiphenyl-4′-yloxy)-ω-(4-cyanobiphenyl-4′-yloxy)alkanes, whereby the number of methylene units in the spacer chain varied from $n=5$ to $n=12$. To quantify the performance of these lasers, the threshold energy and the slope efficiency were extracted from the input-output characteristics of each laser. A clear odd-even effect was observed when both the excitation threshold and the slope efficiency were plotted as a function of the number of methylene units in the spacer chain. In all cases, the bimesogen lasers for which n is even exhibit lower threshold energies and higher slope efficiencies than those for which n is odd. These results are then interpreted in terms of the macroscopic physical properties of the liquid-crystalline compounds. In accordance with a previous study [S. M. Morris, A. D. Ford, M. N. Pivnenko, O. Hadeler, and H. J. Coles, Phys. Rev. E. **74**, 061709 (2006)], a combination of a large birefringence and high order parameters are found, in the most part, to correlate with low-threshold energy and high slope efficiency. This indicates that the threshold and slope efficiency are dominated by the host macroscopic properties as opposed to intermolecular interactions between the dye and the liquid crystal. However, certain differences in the slope efficiency could not be explained by the birefringence and order parameter values alone. Instead, we find that the slope efficiency is further increased by increasing the elastic constants of the liquid-crystal host so as to decrease the scattering losses incurred by local distortions in the director field under high-energy optical excitation.

DOI: 10.1103/PhysRevE.76.051703 PACS number(s): 42.70.Df, 42.70.Qs

I. INTRODUCTION

Photonic band-edge (PBE) lasers formed from liquid-crystal (LC) media are low-threshold microlasers [1]. Chiral LC media which spontaneously self-organize to form a periodic structure exhibit a photonic band gap (PBG) when the periodicity is of the order of the wavelength of light. Within the PBG spontaneous emission is suppressed [2] while at the edges of the PBG strong light localization occurs [3]. With the inclusion of a laser dye, and under optical excitation, low-threshold lasing is achieved at the band edge when the PBG overlaps the spontaneous emission spectrum of the dye. At the band edge, a high density of photon states exists, and this consequently leads to a high gain factor [4]. LC band-edge lasers have a number of benefits ranging from a large coherence area [5] to a micron-sized active gain region. Other features include near-Gaussian beam profile [6], linewidths of the order of 60 pm [7], and wavelength tunability [8–10].

The influence of the macroscopic physical properties of the LC on the laser emission characteristics has been examined, to some extent, in previous studies [11–16]. The birefringence (Δn) [11], orientational order parameter (S_2) [12,13], and order parameter of the transition dipole moment of the dye (S_T) [14,15], have been shown to influence the emission properties of a band-edge laser. Recently, we have reported on a comparison of LC lasers that contained the same gain medium but different nematic hosts [16]. The results indicated that high values of all three parameters (Δn, S_2, S_T) correlated with low-threshold energies and high slope efficiencies. However, for this study a range of different LC hosts were used including monomesogens, nematogen mixtures, and two bimesogens. Therefore, in addition to the variation in the macroscopic physical properties, it is possible that other factors such as intermolecular interactions between the liquid-crystal molecule and the dye in both the ground and excited state may have also influenced the amplification process.

The motivation behind this study was to compare the laser outputs for a range of different LC materials with the same generic molecular structure but very different physical properties. For these reasons, a bimesogenic homologous series was chosen: at the fundamental level these bimesogens consist of two different mesogenic subunits connected by a flexible spacer chain of methylene units. In this case, the generic molecular structure remains the same but the physical properties vary due to the variation in the conformation adopted by the molecules for different spacer lengths. For those containing an odd number of units the molecule assumes a bent configuration compared with those containing even numbers which assume, preferentially, an elongated configuration. The result is the so-called odd-even effect observed in macroscopic properties such as the order parameter and transition temperatures. Using a homologous series of bimesogenic LCs to form lasers, a direct comparison can be made between the host physical properties intrinsic to the LC and the associated laser emission characteristics, e.g., the threshold and slope efficiency. Using expressions for the threshold and slope efficiency derived elsewhere [16] it is shown that the high birefringence and high order parameters do fit with low-threshold and high slope efficiencies. However, results for

*smm56@cam.ac.uk
†Corresponding author. hjc37@cam.ac.uk

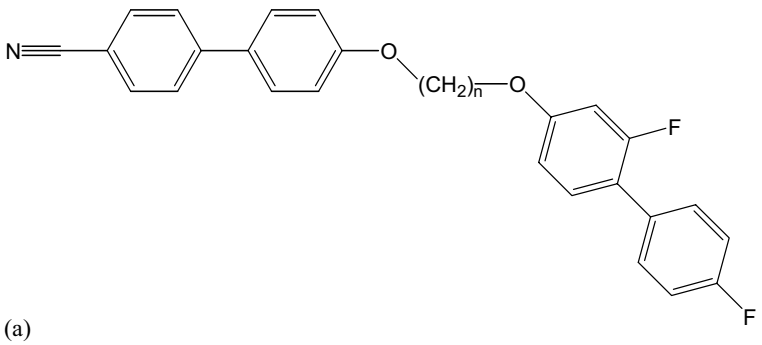

(a)

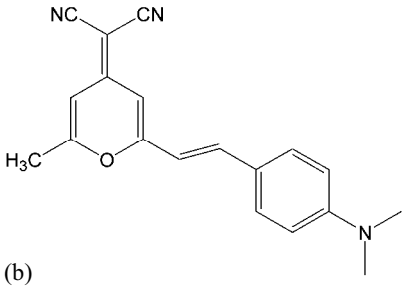

(b)

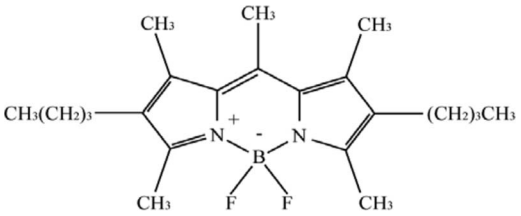

(c)

FIG. 1. The molecular structures of the bimesogen host (a) where n depicts the number of methylene spacer units, (b) the laser dye DCM, and (c) PM597.

the slope efficiency show that other factors must be considered in order to account for the total output. Consequently, we consider other macroscopic LC physical properties that may have an influence on the performance of a LC band-edge laser.

This paper is organized as follows: the materials used and the preparation procedure for the samples is discussed in the following section (Sec. II). Experimental procedure is outlined in Sec. III. Results and discussion are then presented in Sec. IV which is divided into two sections: (a) physical property relations and (b) changing the gain medium. Finally, concluding remarks are made in Sec. V.

II. MATERIALS AND SAMPLE PREPARATION

The nematic hosts used in this study were the nonsymmetric bimesogens belonging to the α-(2′,4-difluorobiphenyl-4′-yloxy)-ω-(4-cyanobiphenyl-4′-yloxy)alkanes homologous series where the number of methylene units in the flexible spacer (n) ranged from 5 to 12; denoted FFOnOCB (synthesized in-house). These molecules consist of an oxy-fluorobiphenyl group and an oxy-cyanobiphenyl group, connected by a flexible spacer chain. The generic molecular structure is shown in Fig. 1. An increase in the number of methylene units, results in a change in the length-to-breadth ratio of each molecule. For the molecules with an odd number of methylene units, it is not energetically favorable for the mesogenic units to align parallel to one another. In contrast, for the molecules with an even number of spacer units, it is energetically favorable for the units to align both parallel and antiparallel in the *all-trans* configuration [17]. This difference in molecular conformation results in different macroscopic LC physical properties for the even-spaced molecules compared with the odd-spaced molecules. The isotropic to nematic phase transition temperatures are plotted as a function of the spacer chain length, n, for the compounds in Fig. 2: note the odd-even effect for T_{IN}.

The two fluorescent dyes chosen for this study were (a) 4-(dicyanomethylene)-2-methyl-6-(4-dimethylaminostryl)-4*H*-pyran, DCM (Lambda Physiks) and (b) 1,3,5,7,8-pentamethyl-2,6-di-*t*-butylpyrromethene-difluoroborate complex, pyrromethene 597 (PM597, Exciton). The molecular structures of DCM and PM597 are also shown in Fig. 1. These two dyes were chosen due to their high fluorescence quantum yield, high miscibility in liquid-crystal media and they could be photoexcited by the second harmonic of an Nd:YAG laser ($\lambda = 532$ nm). DCM exhibits a broad absorbance spectrum with a peak at 470 nm. Due to the similarity in the vibrational energy levels of the ground and the upper laser level, the profile of this broad spectrum is reflected in the emission spectrum with a peak at 600 nm. In comparison, PM597 exhibits narrower absorbance and fluorescence

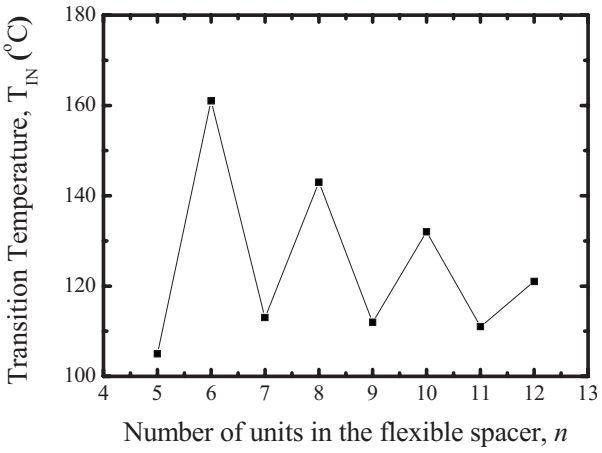

FIG. 2. The isotropic-nematic phase transition temperatures, as a function of the number of methylene units in the spacer chain for the complete homologous series.

spectra than that of DCM with peaks at 530 nm and 590 nm, respectively.

In total, nine PBE-LC laser samples were prepared: eight of which were doped with the DCM dye and one doped with PM597. Each of the eight bimesogenic homologues were doped with a low concentration (3–5 wt. %) of a high twisting power (HTP) chiral dopant (BDH1281, Merck NB-C) and 2 wt. % of DCM. At the long-wavelength band edge, the electric field vector of the LC laser mode is aligned parallel to the local director, compared to the short-wavelength band edge where it is aligned perpendicular. In general, the dye tends to align with the director and therefore the coupling of the laser mode and the dye is maximized at the longer wavelength band edge. A recent report by Huang *et al.* [18] has considered the dependence of the laser threshold energy on the emission wavelength using DCM as the gain medium. It was shown that there was less than 5% variation in the laser threshold energy within the wavelength range of 600 to 620 nm. Consequently, in this study the exact percentage of HTP chiral dopant was determined for each sample in order to position the long-wavelength band edge at 610±10 nm. These eight band-edge lasers were denoted DCM-FFOnOCB* where (n=5–12). The ninth sample consisted of FFO8OCB, 4% BDH1281 and 1.3% PM597, denoted PM597-FFO8OCB*. Once more the percentage of HTP chiral dopant is determined to position the long-wavelength PBE to the dye fluorescence maximum; for PM597 this occurs at 590 nm. The reason that the long-wavelength PBE is positioned to the dye maximum rather than the short-wavelength PBE is because both DCM and PM597 align preferentially to the director and therefore the excitation threshold is lowest at the long-wavelength PBE.

All samples were placed in a bake oven for a minimum period of 24 hours to ensure complete mixing of the constituents through convection processes. The oven was set to a temperature slightly above the nematic to isotropic phase transition temperature. Each sample was capillary filled, in the isotropic phase, into cells with parallel glass walls with 7.5 μm optical path lengths, and inner walls of the cells were coated with a unidirectionally rubbed polyimide alignment layer. Upon cooling the samples, a Grandjean texture was established with the helical axis normal to the glass substrates. The high quality of the alignment was verified using polarizing optical microscopy.

III. EXPERIMENTAL PROCEDURE

In order to photoexcite the bandedge lasers, an Nd:YAG laser (Polaris II, New Wave Research), frequency doubled (532 nm) with half-height pulse widths and a repetition rate of 5 ns and 1 Hz, respectively, was used. Operating frequencies higher than 1 Hz can induce orientational reordering at higher excitation energies thus reducing the quality of the helical structure which can reduce the laser efficiency [19]. The excitation beam was focused onto the sample with an f=10 cm focusing lens to a spot size of 100 μm at the sample, determined using the knife-edge method [20]. Collection optics directed the emitted light to an energy meter (Laserstar, Ophir) and a spectrometer (USB 2000, Ocean Optics) with a spectral resolution of 1.4 nm, for monitoring the lasing wavelength. A 550 nm long-pass filter was employed to remove the excitation beam from the measurements.

The sample was mounted at the focus of the excitation beam on a custom built Linkam hot stage, consisting of a silver block with a built-in heating reservoir, and controlled with a TMS 94 temperature controller to an accuracy of 0.01 °C. A central hole of 1 mm in diameter allowed the full transmission of the excitation laser beam. The hot stage was housed vertically in a three-axis translation holder, built in-house. As a result of the fact that the lasers emit along the axis of the helix in both the forward and backward direction, the emission energies quoted in this paper are multiplied by a factor of 2 to account for the emission in both the forward and backward directions from the cell and are averaged over 25 pulses.

Values for the order parameter of the transition dipole moment of the dye (S_T) were obtained from absorbance measurements using a procedure outlined previously [12]. The birefringence, on the other hand, was measured using an interference technique described elsewhere [21] from which the orientational order parameters were calculated using the Haller technique [22].

IV. RESULTS AND DISCUSSION

A. Physical property relations

Figure 3 shows the input-output characteristics for the odd- (a) and the even- (b) spaced bimesogenic lasers at a shifted temperature of 20 °C. In this case the shifted temperature (T_s) is defined as the difference between the chiral nematic-isotropic clearing temperature (T_c) and the operating temperature (T); $T_s=T_c-T$. For each plot, we observe several features that are synonymous with laser action; an excitation energy threshold, linear excitation-emission characteristics (the slope efficiency) and maximum emission energy (saturation). In the case of the odd-spaced bimesogens, the emission energy is shown up to an excitation energy of 20 μJ/pulse due to a marked decrease in laser emission at higher pulse energies (cf. Ref. [19]) whereas for the even-

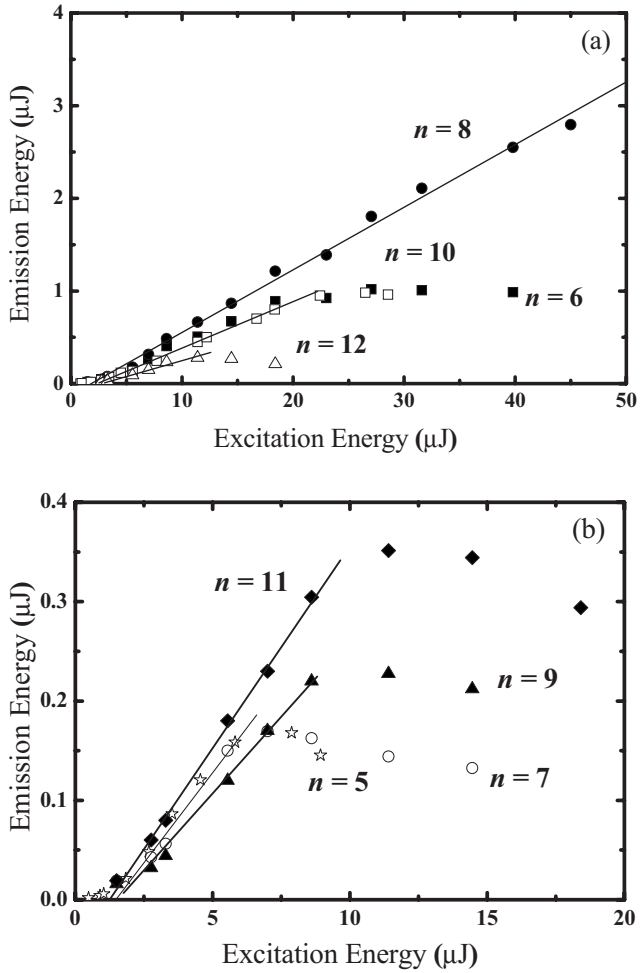

FIG. 3. The input-output characteristics for the odd- (a) and the even- (b) spaced bimesogenic lasers at the same shifted temperature, $T_s = 20$ °C. (a) DCM-FFO5OCB* (☆), DCM-FFO7OCB* (○), DCM-FFO9OCB* (▲), and DCM-FFO11OCB (♦), (b) DCM-FFO6OCB* (■), DCM-FFO8OCB (●), DCM-FFO10OCB (□), and DCM-FFO12OCB (△).

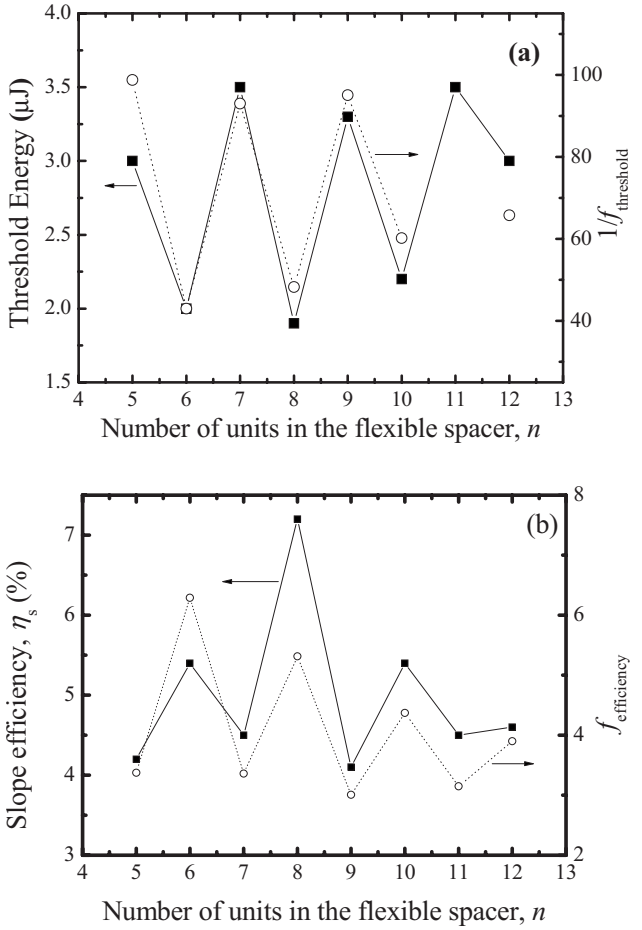

FIG. 4. (a) The laser threshold energy (primary axis) and the *figure-of-merit* parameter (secondary axis) as a function of the number of methylene spacer units, n. (b) The laser slope efficiency (primary axis) and the *figure-of-merit* (secondary axis) as a function of the number of methylene spacer units, n.

spaced bimesogens the emission energy is shown up to an excitation energy of 50 μJ/pulse. Overall the even-spaced lasers exhibit a higher emission energy for any given excitation energy than any of the odd-spaced lasers.

To compare, quantitatively, the performance of the two types of bimesogenic lasers, we consider the dependence of the excitation energy threshold (E_{th}) and the slope efficiency (η_s) on the number of units in the flexible spacer chain. These are shown in Fig. 4, whereby E_{th} is taken as the discontinuity in the differential (cf. Fig. 3) and η_s has been calculated from the roughly linear regime indicated by the straight line fits in Fig. 3. First, we focus on the values of E_{th}. In a similar fashion to that observed for the transition temperatures, a marked odd-even effect is observed. In all cases E_{th} for the odd-spaced bimesogenic lasers is higher than that of the even-spaced bimesogenic lasers. As the length of the spacer chain increases within each odd and even series there is no significant change in E_{th} except for $n=12$. For the mid-length chains, E_{th} is a factor of 1.5 higher for the odd-spaced bimesogenic lasers than for the even-spaced counterparts.

Let us now consider the values of η_s. Figure 4(b) shows that in all cases the slope efficiency of the even-spaced bimesogen lasers is higher than that of the odd-spaced lasers. However, the slope efficiency of DCM-FFO8OCB* appears to be much larger than that of the other even-spaced bimesogenic lasers for the same shifted temperature. Considering, for example, the first three chain lengths ($n=5$, 6, and 7) we see that η_s of DCM-FFO6OCB* is a factor of 1.4 greater than that of its two nearest neighbors. This is also the same for the three bimesogenic lasers containing 9, 10, and 11 methylene units. On the other hand, for the DCM-FFO8OSB* laser, we find that there is a two-fold increase in η_s compared with the two nearest neighboring odd-spaced bimesogenic lasers.

From these results, it is clear that due to the lower threshold and higher slope efficiencies of the even-spaced bimesogenic lasers, their overall performance is better than that of the odd-spaced lasers. Furthermore, the performance appears to peak for the bimesogenic laser containing eight methylene units in the spacer chain. Since the only variant is the number of units in the spacer chain, the change in performance must be due to the change in the physical properties intrinsic to the liquid crystal. In order to explain these results, it is

TABLE I. The material parameters of the bimesogen hosts: the birefringence (Δn), the birefringence at zero Kelvin (Δn_0), the orientational order parameter (S_2), and the order parameter of the transition dipole moment (S_T), for the different bimesogen compounds.

Compound	Δn	Δn_0	S_2	S_T
FFO5OCB	0.2	0.31	0.60	0.3
FFO6OCB	0.24	0.39	0.65	0.37
FFO7OCB	0.2	0.32	0.57	0.32
FFO8OCB	0.24	0.35	0.66	0.39
FFO9OCB	0.19	0.31	0.57	0.35
FFO10OCB	0.23	0.32	0.67	0.38
FFO11OCB	0.19	0.31	0.60	
FFO12OCB	0.21	0.33	0.60	0.39

necessary to examine in more detail the change in the macroscopic properties of the host bimesogen LCs as the spacer length and parity are varied. However, before proceeding, it is first necessary to consider E_{th} and η_s in terms of the macroscopic liquid-crystalline properties.

Through solving the space-independent laser rate equations for a two level system, basic expressions for the laser threshold energy and the slope efficiency in terms of the macroscopic material properties have been obtained previously [16]. These can be written as

$$E_{\text{th}} \propto \frac{1}{\eta_p}\left(\frac{1}{f(S_T)}\right)\left(\frac{1}{f(\Delta n_0)^2 f(S_2)^2}\right), \tag{1}$$

$$\eta_s \propto \eta_p f(\Delta n_0^2) f(S_2^2), \tag{2}$$

where Δn_0 is the birefringence at 0 K, calculated from the extrapolation of the birefringence data to $T=0$ K, S_2 is the orientational order parameter associated with the pseudochiral nematic layers, and S_T is the order parameter of the transition dipole moment of the dye. Δn_0 is a temperature independent term which represents indirectly the anisotropy in the molecular polarizability. That is to say that a large Δn_0 implies a large anisotropy in the molecular polarizability. Each term that includes a LC parameter is written as a function, e.g., $f(S_T)$, since the exact nature of the function is not known explicitly at this stage. However, each function is considered to increase as the corresponding LC parameter increases. The pumping efficiency, η_p, is assumed to be constant across the samples and therefore is excluded from further consideration at this point.

The three LC material parameters, Δn_0, S_2 and S_T, are shown in Table I for a shifted temperature of 20 °C; the birefringence, Δn, is also shown for completeness. Again, for each parameter an odd-even effect is observed whereby values for the even-spaced bimesogens are consistently higher than those of the neighboring odd-spaced bimesogens. To a first approximation, the experimental data in Figs. 3 and 4 can be explained qualitatively in the context of Eqs. (1) and (2): the even-spaced bimesogens exhibit higher Δn_0, S_2, and S_T values than the odd-spaced bimesogens in accord with lower thresholds. The same argument is also valid for the slope efficiency whereby the higher Δn_0 and S_2 values of the even-spaced bimesogens correspond with the higher slope efficiencies.

Following a procedure similar to that carried out in Ref. [16] we define *figure-of-merit* parameters for both the excitation threshold and slope efficiency. These are defined as $f_{\text{threshold}}=(\Delta n_0^2 S_2^2 S_T)\times 100$ and $f_{\text{efficiency}}=\Delta n_0^2 S_2^2$, respectively. The calculated *figure-of-merit* values as a function of the number of methylene units in the flexible spacer chain are also shown in Fig. 4 on the secondary axis. If we consider the calculated values for $f_{\text{threshold}}$ the trend appears to correspond well with the experimental data where the difference in the values of $f_{\text{threshold}}$ between the odd and the even values is a factor of 1.5 which matches that observed for the experimental values of the threshold of the mid-length chains. A decrease in $f_{\text{threshold}}$ at the longer chain lengths is reflected in the E_{th} values and corresponds to the increase in molecular flexibility as the chain length increases.

In contrast, the calculated values of $f_{\text{efficiency}}$ only partially follow the measured values of η_s with the obvious discrepancy of the DCM-FFO8OCB* laser. This homologue notwithstanding, $f_{\text{efficiency}}$ is found to be 1.4 times larger for the even-spaced molecules compared with that of the odd-spaced molecules. The value of FFO12OCB is found to be lower due to smaller values of the birefringence and order parameters and hence the corresponding value of η_s is also smaller.

The change in the excitation threshold and slope efficiency can be explained, to some extent, in the context of the relationships of Eqs. (1) and (2) in combination with the results for the material parameters of the host liquid-crystalline medium. However, there is one anomaly that these physical parameters do not account for; the extraordinarily high slope efficiency of DCM-FFO8OCB*. This same feature was reported in a previous study [16]. Both FFO6OCB and FFO8OCB have very similar birefringences and therefore we would expect the density of photon states to be approximately the same. This indicates that the density of photon states alone does not determine the overall output of the LC laser.

Factors such as the dye concentration and cell thickness are not varied during measurements and thus cannot be responsible for the marked change in performance. It is interesting to note that whatever factor is responsible for the large slope efficiency does not appear to influence the threshold. Samples were prepared through a careful annealing procedure which resulted in a large single chiral nematic planar monodomain. Therefore, light localization due to inhomogenieties in the refractive index, resulting from polydomains, was not considered to be a potential factor as each sample was carefully prepared before measurements in order to form such a monodomain. It is also unlikely that the quantum efficiency was different given that the generic molecular structure remains the same. Using the same reasoning, it is also unlikely that the absorption cross section varies significantly either. This would result in a change in the pump efficiency and would in turn lead to a reduction in the excitation threshold which was not observed. Other possible factors include thermal conductivity and absolute temperatures: typically, the fluorescence quantum yield decreases at high temperatures. However, these factors are not considered to

be the cause given that the even-spaced bimesogen lasers are the ones that are operated at higher absolute temperatures.

A further important factor could be the elastic restoring force of the chiral nematic LC host. Under high-energy photoexcitation the liquid-crystal medium can become distorted due to angular momentum transfer between the electromagnetic field and the dye-doped liquid-crystalline medium: the presence of the dye leads to an additional photoinduced torque that significantly enhances the total optical torque through a phenomenon known as the Jánossy effect [23]. As a result of the local perturbations in the director field, the Q factor of the overall resonator would decrease. The magnitude of the local perturbations in the director field is governed by the magnitude of the elastic constants: large values of the elastic constant result in small director distortions; this is discussed in more detail shortly. For arguments sake, we refer to the resistive element of the helical structure of the chiral nematic to optical field and thermal-induced distortions as the structural integrity of the cavity.

Measurements for the splay elastic constant, K_{11}, have been obtained for each bimesogen host by recording the Fréedericksz threshold voltage, V_{th}, using planar aligned cells. The splay elastic constant can then be extracted from the following relationship if the dielectric anisotropy, $\Delta\varepsilon$, is known:

$$K_{11} = \frac{V_{\text{th}}^2 \varepsilon_0 \Delta\varepsilon}{\pi^2}. \tag{3}$$

The method used for determining the dielectric anisotropy of the bimesogen compounds is discussed elsewhere [24]. The results are shown in Fig. 5(a), where it can be seen that K_{11} for $n=8$ is larger than for the other homologues. Due to the fact that a reliable homeotropic alignment cannot be achieved using the bimesogens, measurements of the twist and bend elastic constants using dynamic light scattering have not been possible. However, we can qualitatively assess the magnitude of the twist elastic constant indirectly by noting the concentration of chiral additive required to position the long-wavelength band edge at 610 nm. Figure 5(b) shows that the concentration required was much higher for FFO8OCB than any of the other compounds indicating that the twist elastic constant is much higher than for the other homologues.

We now consider the relationship between the elastic constants and fluctuations in the director field in more detail. It is well known that a distortion or fluctuation in the director field of a chiral nematic LC is the primary mechanism behind light scattering [25]. Director fluctuations give rise to fluctuations in the local dielectric constant which in turn gives rise to light scattering. There are two principle types of distortion for a chiral nematic LC, the twist mode and the conical (or umbrella) mode [26]: the direction of the wave vector for both these modes points along the helix axis, these modes are illustrated in Fig. 6. For the twist mode the fluctuation of the director is perpendicular to the wave vector of the helix and can be thought of as a modulation in the phase of the helical structure. In contrast, for the umbrella mode the fluctuations in the director are parallel to the wave vector

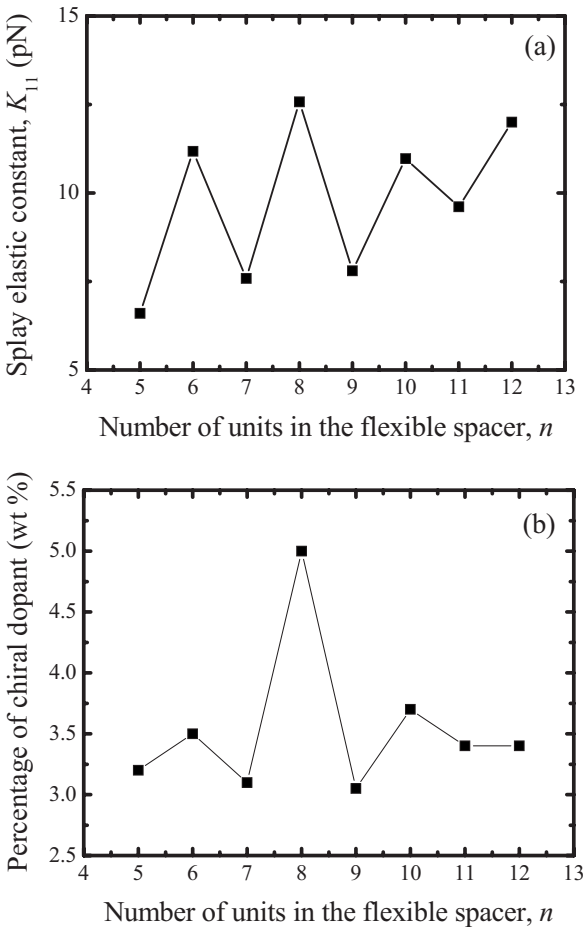

FIG. 5. (a) The splay elastic constant as a function of the number of units in the flexible spacer, n. (b) The chiral dopant percentage required to position the long-wavelength band edge at a wavelength of 610 ± 10 nm as a function of the number of methylene units in the spacer chain, n.

and involve a modulation of the tilt of the director away from its preferred direction perpendicular to the helix axis.

In actual fact, there are three additional modes which also account for the wave vector being perpendicular to the helix axis. However, the twist and the umbrella modes tend to dominate over the other modes when considered at a temperature far from the clearing temperature (i.e., away from the pretransitional region); a result of the substantially larger intensity of the light scattered by distortions in contrast to that occurring from fluctuations in the LC density [27]. In this study, the laser emission is examined at a shifted temperature of 20 °C and thus these two principle modes, twist and umbrella, are the only two to be considered further.

The average square fluctuations for each of the two primary modes, twist and umbrella, respectively, can be written as [26]

$$\langle |\delta n(k)|^2 \rangle = \frac{k_B T}{K_{22} k^2}, \quad k = q \pm 2q_0 \tag{4}$$

and

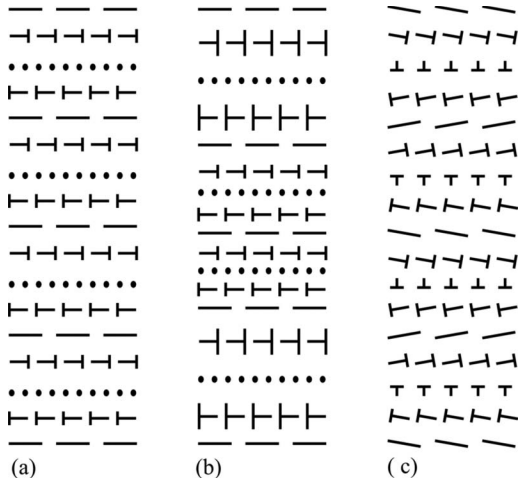

FIG. 6. Illustrations of the director profile for the fundamental deformations of a chiral nematic liquid crystal: (a) unperturbed chiral nematic, (b) twist mode, and (c) umbrella mode. The nails represent inclinations with respect to the page, Ref. [26].

$$\langle |\delta n(k)|^2 \rangle = \frac{k_B T}{K_{33} q_0^2 + K_{11} k^2}, \quad k = q \pm q_0, \tag{5}$$

where δn denotes the director fluctuation, q_0 is the wave vector, k_B is the Boltzmann constant, T is the temperature, and K_{11}, K_{22}, K_{33} are the splay, twist and bend elastic constants, respectively. These expressions have been derived by applying the equipartition theorem to the Frank free energy for director distortions.

According to Eq. (4), which represents the twist mode, a LC with a large twist elastic constant, K_{22}, will only give rise to small director fluctuations and consequently the intensity of the light scattered will be low [27]. Likewise, the scattered intensity for the umbrella mode is determined by K_{11} and K_{33}. Scattering losses are a source of drain for a laser cavity and serve to reduce the overall efficiency of the laser. Consequently, larger values of the elastic constants would be preferable in order to reduce the director fluctuations and thus reduce the scattering losses from the cavity. We believe, therefore, that the higher slope efficiency observed for the laser DCM-FFO8OCB* is a result of the fact that the bimesogenic host exhibits larger elastic constants.

In further support of this hypothesis are the results presented in Fig. 3 where it can be seen that the point of saturation corresponds to an excitation energy significantly larger for DCM-FFO8OCB* than for any of the other homologues. In the case of DCM-DCM-FFO8OCB*, the point of saturation exceeds an excitation energy of 50 μJ/pulse whereas, in contrast, the remaining homologues have already reached their saturation limit at considerably lower excitation energies; 10–20 μJ/pulse.

The structural integrity explanation, however, requires further comment. If we take this through to a logical conclusion we might expect that the threshold energy would also be affected by the elastic constants. To a first approximation, $\eta_s \propto 1/\Gamma$, where Γ represent the loss mechanisms and therefore low scattering losses would lead to high slope efficiency.

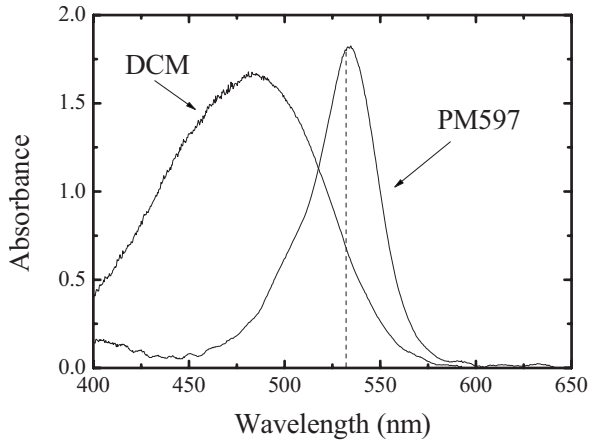

FIG. 7. The absorbance of DCM (solid curve) and PM597 (dashed curve) in FFO8OCB at a shifted temperature of 20 °C. The vertical dotted line indicates the pump wavelength.

For a conventional Fabry-Perot cavity scattering losses directly influence the laser threshold, however, for the LC laser the situation is slightly different. The coupling between the electromagnetic field and the dielectric anisotropy of the medium can generate local disturbances in the director field which then scatter light due to inhomogeneities in the refractive index. However, this photoinduced director distortion may actually only occur at energies above the threshold and therefore this type of scattering loss would not influence the excitation threshold directly. Larger elastic constants result in lower scattering intensities and thus restrict photoinduced director reorientation to higher input energies. This is reinforced by the results presented both herein and elsewhere [16] which show that the saturation limit occurs at different energies for different liquid crystals containing the same dye. Consequently, the result is thus not due to thermal or photoinduced degradation.

B. Changing the gain medium

As a test of our conclusions concerning the important role of the host properties, we decided to examine further the emission characteristics for the $n=8$ high slope efficiency bimesogenic laser doped with an alternative dye that has a higher absorbance at $\lambda = 532$ nm, namely PM597. Although DCM does absorb at the excitation wavelength ($\lambda = 532$ nm), its absorbance maximum is positioned at 470 nm. PM597, on the other hand, has a maximum absorbance in LC media that is located much closer to the excitation wavelength as is shown in Fig. 7. An increase in the absorbance of the excitation wavelength should result in an increase in the pump efficiency, η_p, and consequently according to Eqs. (1) and (2), a decrease in the threshold with a simultaneous increase in the slope efficiency. At $\lambda = 532$ nm, $A = 1.8$, and $A = 0.7$, for PM597 and DCM, respectively. It should be noted that the increase in the absorbance is not the only change since the order parameter S_T and the quantum efficiency will also change. Furthermore, the intermolecular interactions will also be different due to the different molecular structure of the dye.

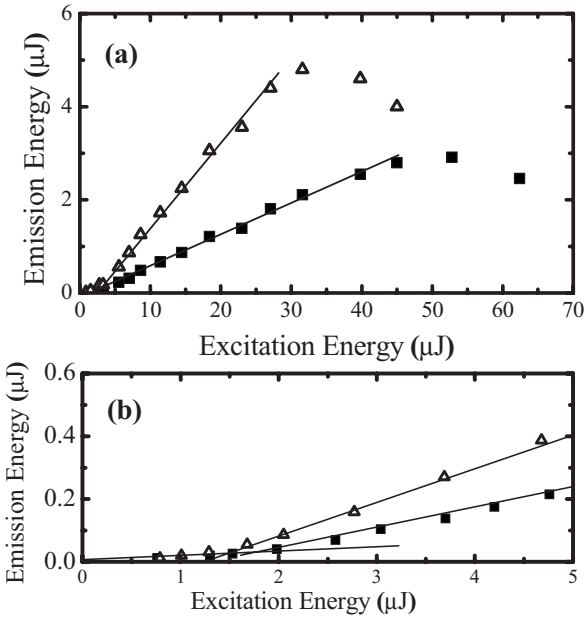

FIG. 8. (a) The input-output characteristics of DCM-FFO8OCB* (■) and PM597-FFO8OCB* (△) and (b) the corresponding threshold energies of DCM-FFO8OCB* (■) and PM597-FFO8OCB* (△).

Figure 8 shows the input-output characteristics of the two lasers, DCM-FFO8OCB* and PM597-FFO8OCB*, at a shifted temperature of 20 °C. The results show the emission energy for DCM-FFO8OCB* up to an excitation energy of 70 μJ/pulse, whereas for PM597-FFO8OCB* the emission energies are recorded up to an excitation energy of 50 μJ/pulse. This is due to the fact that PM597-FFO8OCB* reaches saturation at a lower excitation energy than DCM-FFO8OCB*, although with higher emission energies. Measurements of the threshold energies were performed over the excitation energy range of 0–5 μJ/pulse, Fig. 8(b). By virtue of the fact that the fluorescence peak and hence gain maximum of PM597 occur at a shorter wavelength than DCM, the two bimesogenic lasers therefore emit at different wavelengths, $\lambda_{PM597}=590$ nm and $\lambda_{DCM}=610$ nm. It is shown that the emission energies for any given excitation energy for PM597-FFO8OCB* are consistently higher than those of DCM-FFO8OCB*. From the data we find that the threshold and slope efficiencies for PM597-FFO8OCB* are 1.5 μJ/pulse and 18%, respectively, compared with 1.9 μJ/pulse and 7% for DCM-FFO8OCB*.

According to Eq. (1), E_{th} is inversely proportional to the three LC material parameters as well as the pump efficiency. For each bimesogenic laser the host remains constant, and hence the values of Δn_0 and S_2 are considered to be unchanged, with values of 0.35 and 0.66 accordingly. It should be noted that while Δn_0 does depend upon wavelength, the difference in magnitudes for $\lambda=590$ nm and $\lambda=610$ nm is considered to be small. For simplicity, the effect on E_{th} and η_s is then considered to be negligible. Consequently, in this case E_{th} is found to be inversely proportional to η_p and S_T only. Calculations of S_T from the absorbance parallel and perpendicular to the director provided values for PM597-FFO8OCB of $S_T=0.45$ whereas values for DCM-FFO8OCB of $S_T=0.39$. From Eq. (1), a combined increase in the values of S_T and η_p will result in a reduction in E_{th}. The results show that E_{th} for PM597-FFO8OCB* is lower than that of DCM-FFO8OCB* by a factor of 0.2. Thus a reduction in E_{th} is observed although it is not of the same order of magnitude as that observed for the combined increase in the absorbance and S_T.

Equation (2) implies that η_s is linearly dependent on η_p only, assuming all other factors are equal. To a first approximation the pump efficiency can be considered to be proportional to the absorption cross section, σ_a, and the number of molecules in the ground state, N_0. According to the Beer-Lambert law, in the absence of scattering, the absorbance can be expressed as $A=\sigma_a dc$ where d is the path length and c is the molar concentration. If we assume that the path length and the concentration remain constant the change in η_p is due exclusively to a change in σ_a and consequently A. Therefore, a 2.6-fold increase in A would result in an enhancement of the slope efficiency by the same order of magnitude, assuming a concomitant increase in σ_a. This is indeed what is observed.

A further factor of interest is the different saturation limit observed for the two DCM and PM597 based lasers. It can be seen that the saturation limit occurs at a lower excitation energy for the PM597-FFO8OCB* laser ($E_{\text{exc}}\sim 32$ μJ/pulse) compared with the DCM-FFO8OCB* laser ($E_{\text{exc}}\sim 53$ μJ/pulse). If the excitation energy corresponding to the saturation limit was directly related to the elastic moduli of the liquid-crystal host, one might at first expect the saturation limits to occur at the same excitation energy irrespective of the gain medium. However, the amount of energy absorbed by the dye-doped LC differs for the two lasers, which must be taken into account. Furthermore, the energy contained within the liquid-crystal laser mode also differs and it is the combined energy which must be considered. The situation is further complicated by the fact that photoinduced director reorientations can occur at different threshold energies depending upon the dye structure and its alignment with the LC matrix. We are currently carrying out further research in this area to gain a better understanding of all the factors involved and what determines the saturation limit.

V. CONCLUSIONS

Band-edge lasing from a homologous series of nonsymmetric bimesogen liquid crystals has been studied. For both the excitation energy threshold and slope efficiency a strong odd-even effect is observed when plotted as a function of the number of methylene units in the flexible spacer chain of the host bimesogen. The even-membered homologues give higher slope efficiencies and lower threshold energies than the odd homologues. By considering the macroscopic properties of the liquid crystal, such as the birefringence and the order parameters, we find a qualitative explanation for the dependence of the excitation threshold on the chain length of the bimesogen host. However, it is found that these properties alone cannot be used to fully explain the dependence of the slope efficiency on the length of the spacer chain. One bimesogen laser ($n=8$), in particular, appears to exhibit a

much higher slope efficiency than the other lasers despite having similar values for the birefringence and the order parameters, as well as the same gain medium and concentration thereof. For these reasons we have considered which other properties are potentially of importance in the lasing process. It is suggested that, by virtue of the high sensitivity of liquid crystals to electric fields, that the elastic properties must also be of importance. Our reasoning is based on the fact that, during optical pumping, intense optical fields exist in the liquid-crystal medium which can generate local distortions in the director field through coupling with the dielectric properties: an effect which is enhanced when a dye is present. The resistance to a distortion in the director field is governed by the elastic constants whereby larger magnitudes lead to higher Q factors.

ACKNOWLEDGMENTS

The authors thank the EPSRC for support of this work through COMIT Faraday Partnership CASE program with Dow Corning (A.D.F.) and Merck NB-C (C.G.). One of the authors (H.J.C.) gratefully acknowledges the financial support of the Basic Technology Research Grant COSMOS (Grant No. EP/D4894X/1, EPSRC, UK).

[1] V. I. Kopp, B. Fan, H. K. M. Vithana, and A. Z. Genack, Opt. Lett. **23**, 1707 (1998).
[2] E. Yablonovitch, Phys. Rev. Lett. **58**, 2059 (1987).
[3] S. John, Phys. Rev. Lett. **58**, 2486 (1987).
[4] J. P. Dowling, M. Scalora, M. J. Bloemer, and C. M. Bowden, J. Appl. Phys. **75**, 1896 (1994).
[5] V. I. Kopp, Z. Q. Zhang, and A. Z. Genack, Phys. Rev. Lett. **86**, 1753 (2001).
[6] V. I. Kopp, Z. Q. Zhang, and A. Z. Genack, Prog. Quantum Electron. **27**, 369 (2003).
[7] S. M. Morris, A. D. Ford, B. J. Broughton, M. N. Pivnenko, and H. J. Coles, Proc. SPIE **5741**, 118 (2005).
[8] P. V. Shibaev, R. Lea Sanford, D. Chiappetta, V. Milner, A. Genack, and A. Bobrovsky, Opt. Express **13**, 2358 (2005).
[9] Y. Huang, Y. Zhou, and S.-T. Wu, Appl. Phys. Lett. **88**, 011107 (2006).
[10] M. Ozaki, M. Kasano, T. Kitasho, D. Ganzke, W. Hasse, and K. Yoshino, Adv. Mater. (Weinheim, Ger.) **15**, 974 (2003).
[11] M. G. Chee, M. H. Song, D. Kim, H. Takezoe, and I. J. Chung, Jpn. J. Appl. Phys., Part 2 **46**, L437 (2007); S. M. Morris, A. D. Ford, M. N. Pivnenko, and H. J. Coles, Proc. SPIE **5289**, 236 (2004).
[12] S. M. Morris, A. D. Ford, M. N. Pivnenko, and H. J. Coles, J. Appl. Phys. **97**, 023103 (2005).
[13] P. V. Shibaev, V. Kopp, A. Genack, and E. Hanelt, Liq. Cryst. **30**, 1391 (2003).
[14] J. Schmidtke and W. Stille, Eur. Phys. J. B **31**, 179 (2003).
[15] F. Araoka, K.-C. Shin, Y. Takanishi, K. Ishikawa, Z. Zhu, T. M. Swager, and H. Takezoe, J. Appl. Phys. **94**, 279 (2003).
[16] S. M. Morris, A. D. Ford, M. N. Pivnenko, O. Hadeler, and H. J. Coles, Phys. Rev. E **74**, 061709 (2006).
[17] A. Ferrarini, G. R. Luckhurst, P. L. Nordio, and S. J. Roskilly, Chem. Phys. Lett. **214**, 409 (1993).
[18] Y. Huang, Y. Zhou, and S.-T. Wu, Appl. Phys. Lett. **88**, 011107 (2006).
[19] S. M. Morris, A. D. Ford, and M. N. Pivnenko, J. Opt. A, Pure Appl. Opt. **7**, 215 (2005).
[20] See, for example, R. Menzel, *Photonics: Linear and Nonlinear Interactions of Laser Light and Matter* (Springer-Verlag, Berlin, Heidelber, 2001).
[21] R. Chang, Mater. Res. Bull. **7**, 267 (1972).
[22] I. Haller, Prog. Solid State Chem. **10**, 103 (1975).
[23] I. Jánossy, A. D. Lloyd, and B. S. Wherrett, Mol. Cryst. Liq. Cryst. **179**, 1 (1990).
[24] S. M. Morris, M. J. Clarke, A. E. Blatch, and H. J. Coles, Phys. Rev. E **75**, 041701 (2007).
[25] P. de Gennes and J. Prost, *The Physics of Liquid Crystals* (Clarendon, Oxford, 1993).
[26] M. A. Pantea and P. H. Keyes, Phys. Rev. E **71**, 031707 (2005).
[27] S. Chandrasekhar, *Liquid Crystals*, 2nd ed. (Cambridge University Press, Cambridge, 1992).